Food & Function

Accepted Manuscript

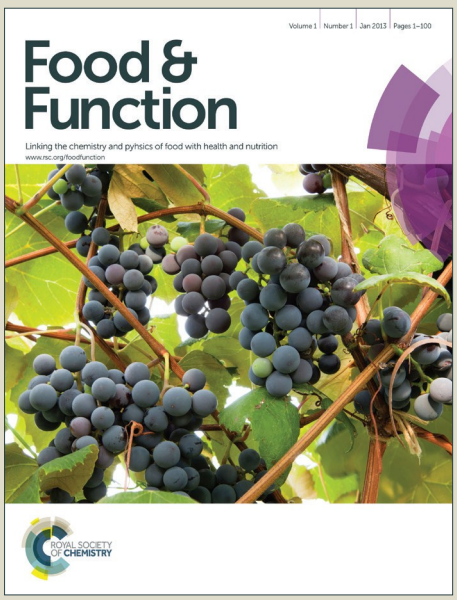

This is an *Accepted Manuscript*, which has been through the Royal Society of Chemistry peer review process and has been accepted for publication.

Accepted Manuscripts are published online shortly after acceptance, before technical editing, formatting and proof reading. Using this free service, authors can make their results available to the community, in citable form, before we publish the edited article. We will replace this *Accepted Manuscript* with the edited and formatted *Advance Article* as soon as it is available.

You can find more information about *Accepted Manuscripts* in the Information for Authors.

Please note that technical editing may introduce minor changes to the text and/or graphics, which may alter content. The journal's standard Terms & Conditions and the Ethical guidelines still apply. In no event shall the Royal Society of Chemistry be held responsible for any errors or omissions in this *Accepted Manuscript* or any consequences arising from the use of any information it contains.

ROYAL SOCIETY OF CHEMISTRY

www.rsc.org/foodfunction

Inhibitory mechanism of morin on α-glucosidase and its anti-glycation properties

Li Zeng [a], Guowen Zhang [a,*], Yijing Liao [a], Deming Gong [b]

[a] State Key Laboratory of Food Science and Technology, Nanchang University, Nanchang 330047, China

[b] School of Biological Sciences, The University of Auckland, Auckland 1142, New Zealand

[*] Corresponding author: Professor Guowen Zhang, Ph.D., Tel: +86-791-88305234, fax: +86-791-88304347. *E–mail address*: gwzhang@ncu.edu.cn

ABSTRACT

It is important to investigate the inhibition of α-glucosidase due to its correlation with type 2 diabetes. Morin was found to exert a significant inhibition activity on α-glucosidase in a reversible mixed−type manner with an IC_{50} value of (4.48 ± 0.04) μM. Analyses of fluorescence and circular dichroism spectra indicated that the formation of morin−α-glucosidase complex was driven mainly by hydrophobic forces and hydrogen bonding, and caused the conformational changes of α-glucosidase. The phase diagrams of fluorescence showed that the conformational change process was monophasic without intermediates. Molecular docking indicated that morin mainly interacted with amino acid residues located close to the active site of α-glucosidase, which may move to cover the active pocket to reduce the binding of substrate and then inhibiting the catalytic activity. Morin was also found to exhibit inhibition on the generation of advanced glycation endproducts which was related to the long term complications of diabetes.

Keywords: α-Glucosidase; Morin; Inhibition mechanism; Anti-glycation; Multispectroscopic methods; Molecular docking.

1. Introduction

Diabetes mellitus (DM) is a serious problem worldwise and intensive study is urgently needed, because it would become 7th leading cause of death globally by the year 2030 predicted by the World Health Organization (WHO).[1] DM is a chronic metabolic disorder which is associated with a congenital (DM1) or acquired (DM2) inability to transport glucose from the bloodstream into cells generating a high level of glucose in the blood.[2] The reducing sugars can react with amino groups in proteins and ultimately promote the irreversible formation of reactive advanced glycation endproducts (AGEs). This process is known as non-enzymatic glycation which has been reported to play a vital role in the long term complications of diabetes.[3] If this disease receives no duly and effectively treatments, it will cause diabetic complications, such as hyperglycemia, diabetic heart disease, diabetic ketoacidosis or nonketotic hyperosmolar coma.[4] At present, the underlying mechanisms of anti-hyperglycemic activities are mainly regarded as the inhibition of carbohydrate digestive enzymes, such as α-glucosidase, and α-amylase, and anti-glycation activities.[5]

α-Glucosidase is intestinal brush border membrane-bound enzyme which contributes to catalyze the reactions related to the carbohydrate digestion. The enzyme hydrolyzes α-(1-4)-linked D-glucose residues from the non-reducing end,[6] and leads to the digestion of polysaccharides and disaccharides. α-Glucosidase activity has been considered as the primary factor related to DM. Hence, suppressing the activity of α-glucosidase is an effective treatment approach of DM2. α-Glucosidase inhibitors decrease the activity of enzyme and retard the digestion of carbohydrates, which would delay and reduce the level of postprandial hyperglycaemia.[7] Some drugs such as acarbose, voglibose and miglitol are the commonly used α-glucosidase inhibitors to

treat DM2 in clinic,[8] but they were reported to lead to some undesirable side effects, for instance, flatulence, stomachache, diarrhoea and liver damage.[9] Aminoguanidine is the first synthetic anti-glycation agent tested in clinical trials to alleviate diabetic complications, however it is a hydrazine derivative and causes systemic toxicity upon long-term intake.[10] Therefore, to search for more effective and safe α-glucosidase inhibitors is in great demand. Due to the low toxicity of herbs in nature, discovering natural compounds from herbs that can not only act as α-glucosidase inhibitors but feature with anti-glycation has become an important approach in the treatment of DM2 with dual action.

Dietary flavonoids, naturally occurring phenolic compounds, are widely distributed in various foods and plants including tea, wine, fruit and vegetables.[11] Recently, dietary flavonoids have attracted growing attention because of their therapeutic activities, for example, potential antidiabetic agents.[11] Morin (structure shown in Figure 1A), 3, 5, 7, 2', 4'-pentahydroxyflavone, is abundant in plants and foods of plant origin especially in seaweeds, onion and guava leaves.[12] Perevious studies have reported the contents of morin in seaweeds ranging from 257 ± 25 to 3730 ± 23 μg/g dry weight [13] and the total flavonoids contents varying from 7.41 ± 0.49 to 42.50 ± 0.86 mg QE/g.[14] The highest amount of total flavonoids contents in twelve cultivars of different colored onions was 979.1 mg/kg on fresh material in *"Dorata Density"*.[15] The total flavonoids contents in white guava and red guava were determined to be 19.06 and 35.85 mg CE/100g.[16] Morin was found to exhibit various pharmacological activities including antioxidant, antinociceptive, antitumor, antiinflammatory and cardioprotective effects.[17] Although morin has been reported to exert the inhibition on α-glucosidase activity,[18] the study was restricted to the enzymatic activity assay, the underlying inhibition mechanism of morin on α-glucosidase is still unclear, and there

is little information on its anti-glycation activity.

In this study, we used multispectroscopic methods including UV−vis absorption, fluorescence and circular dichroism (CD) combined with molecular docking to investigate the inhibitory kinetics, anti-glycation and interaction mechanism of morin on α-glucosidase. The half inhibitory concentration (IC_{50}), inhibition type, inhibition constant and thermodynamic parameters were determined. The special binding site and conformational change of α-glucosidase were evaluated to determine the inhibition mechanism of morin on the enzyme.

2. Materials and methods

2.1. Materials

α-Glucosidase (EC 3.2.1.20) from *Saccharomyces cerevisiae* obtained from Sigma-Aldrich Co.(St, Louis, USA) was dissolved in sodium phosphate buffer (0.1 M, pH 6.8). Acarbose and p-nitrophenyl-α-D- glucopyranoside (*p*NPG), purchased from Sigma-Aldrich Co. (St. Louis, MO, USA), were both dissolved in sodium phosphate buffer to prepare their stock solutions with concentrations of 5.0 and 9.1 mM respectively. Morin (analytical grade) was from Aladdin Chemistry Co. (Shanghai, China), and its stock solution (5.0 mM) was made in dimethyl sulfoxide (DMSO) then to the specified volume by adding ultrapure water. The content of DMSO in this work was below 0.5% with no effect on the activity of α-glucosidase. Bovine serum albumin (BSA), purchased from Sino-American Biotechnology Co. (Luoyang, China), and fructose were dissolved in potassium phosphate buffer (0.2 M, pH 7.4, containing 0.06% sodium azide). Aminoguanidine hydrochloride (AG) was from Sinopharm Chemical Reagent Co. (Shanghai, China). All other reagents were of analytical reagent grade, and the ultrapure water was used throughout the whole experiment.

2.2. α-Glucosidase activity assay

The α-glucosidase inhibitory activity of morin was evaluated by using the method of Ohta et al.[19] with slight alteration. The reaction system contained a series of different concentrations of morin, a fixed concentration of α-glucosidase (50.8 nM) and a certain quantity of sodium phosphate buffer (0.1 M, pH 6.8). Then the mixtures were incubated for 2 h at 37 ºC to make the reaction equilibrium. *p*NPG (final concentration 454 μM) was added to the morin−enzyme complex solution to initiate the reaction, and the final volume of the reaction system was kept at 2 mL. The enzymatic activity of α-glucosidase was determined by measuring the absorption at 405 nm every 5 s on a Persee TU−1901 double beam UV−vis spectrophotometer (Persee, Beijing, China) with 1.0 cm quartz cells. Acarbose was used as a positive control. The inhibitory effect of morin on α-glucosidase was defined as relative enzymatic activity (%) = (slope of reaction kinetics equation obtained by reaction with inhibitor)/(slope of reaction kinetics equation obtained by reaction without inhibitor) × 100.

2.3. In vitro glycation assay

The assay was used to investigate the inhibitory effect of morin on the formation of AGEs with the method of Wang et al.[20] Briefly, a series of assay solutions containing fixed concentration of BSA (20 mg mL^{-1}), fructose (0.5 M) and different concentrations of morin in potassium phosphate buffer (0.2 M, pH 7.4, containing 0.06% sodium azide) were incubated at 50 ºC for 24 h. The fluorescence spectra were recorded from 385 to 600 nm at the excitation of 360 nm on a Model F−7000 Hitachi spectrofluorimeter (Hitachi, Japan) equipped with a 150 W xenon lamp and a thermostat bath. Both the excitation and emission slits were set at 5.0 nm. The inhibition of protein glycation was interpreted as relative anti-glycative activity (%) = [(fluorescence of control − fluorescence of test sample)/fluorescence of control]

146 ×100.[20] AG was used as a positive control.

147 **2.4. Analysis of inhibitory kinetics**

148 The same method as α-glucosidase activity assay was used to determined the type of
149 inhibition of morin to α-glucosidase. To analyze the mixed−type inhibition
150 mechanism, the Lineweaver−Burk equation can be written in double reciprocal form:
151 [21]

152 $$\frac{1}{v}=\frac{K_{\mathrm{m}}}{V_{\max}}(1+\frac{[I]}{K_{\mathrm{i}}})\frac{1}{[S]}+\frac{1}{V_{\max}}(1+\frac{[I]}{K_{\mathrm{is}}}) \quad (1)$$

153 Secondary plots were constructed from

154 $$Slope=\frac{K_{\mathrm{m}}}{V_{\max}}+\frac{K_{\mathrm{m}}[I]}{V_{\max}K_{\mathrm{i}}} \quad (2)$$

155 and

156 $$Y\text{ - intercept}=\frac{1}{V_{\max}^{\mathrm{app}}}=\frac{1}{V_{\max}}+\frac{1}{K_{\mathrm{is}}V_{\max}}[I] \quad (3)$$

157 where K_{i} *and* K_{is} represent the equilibrium constant for binding with free enzyme and
158 enzyme−substrate complex, respectively, and K_{m} is Michaelis−Menten constant. v is
159 the enzyme reaction rate in the absence and presence of morin. The secondary re-plot
160 of Slope or Y-intercept *vs*. [I] was linearly fitted, implying a single inhibition site or a
161 single class of inhibition sites.[22]

162 **2.5. Fluorescence spectra measurements**

163 The α-glucosidase (1.0 μM) was titrated successively with varying concentration of
164 morin from 0 to 21.07 μM. The mixtures were stood for 3 minutes to equilibrate, and
165 the fluorescence emission spectra were then measured at 292, 298 and 310 K from
166 300 to 500 nm upoon excitation 280 nm. Both the excitation and emission bandwidths
167 were set at 2.5 nm. Appropriate blanks corresponding to the sodium phosphate buffer
168 were subtracted to correct background fluorescence.

Synchronous fluorescence spectra were obtained from 200 to 400 nm by setting the excitation and emission wavelength interval (Δλ) at 15 and 60 nm, at which the spectrum only showed the spectroscopic behavior of tyrosine and tryptophan residues of α-glucosidase, respectively.

Because the absorption of excited light and the re-absorption of emitted light would cause the deviation of fluorescence value, so the following relationship was used to correct the inner-filter effect: [23]

$$F_c = F_m e^{(A_1+A_2)/2} \quad (4)$$

where F_c and F_m indicate the corrected and measured fluorescence, respectively. A_1 and A_2 represent the absorbance of morin at excitation and emission wavelengths, respectively.

2.6. CD spectroscopy

The CD spectra were recorded on a Bio−Logic MOS 450 CD spectrometer (Bio-Logic, Claix, France) in the far−UV region (190−250 nm) under constant nitrogen flush using the 1.0 mm path length cuvette and in the near−UV region (250−350 nm) using the 1.0 cm path length cell. The molar ratios of morin to α-glucosidase were 0:1, 4:1 and 6:1 in the far−UV CD spectra and 0:1, 2:1, 4:1 and 6:1 in the near−UV CD spectra. All recorded CD spectra were measured in sodium phosphate buffer (0.1 M, pH 6.8) at room temperature with a fixed concentration of α-glucosidase (2.0 μM) and the buffer signal was subtracted. The contents of different secondary structures of α-glucosidase were analyzed by the online SELCON3 program (http://dichroweb.cryst.bbk.ac.uk/html/home. shtml).

2.7. Docking simulation

In order to explore the probable interaction between morin and α-glucosidase, the docking program AutoDock (vers.4.2) was used as a supplement. No

three-dimensional structural information is currently available for the eukaryotic α-glucosidase from *Saccharomyces cerevisiae*. Using BLAST algorithms with the amino acid sequence of the target as input, the Protein Data Bank (PDB) from the protein sequence data bank (http://www.ncbi.nlm.nih.gov/protein/) was searched to find a proper structural template for homology modeling. The 3D structure of morin was formed in Chem3D Ultra 8.0. The homology model was used as the receptor model in the virtual screening with AutoDock (version 4.2).[24] The dimension of grid box was set to 80Å × 86Å × 100Å with a spacing of 0.375Å. Lamarckian genetic algorithm (LGA) was used to execute the docking calculations, and the search parameters were set for 100 times.

2.8. Statistical analysis

All the data were analyzed by using the SAS statistical package (version 8.1, SAS Institute, Cary, NC, USA). The results were expressed as the mean values ± standard deviation ($n = 3$). One−way analysis of variance (ANOVA) was implemented by using Origin 8.0 followed by multiple tests in order to determine the significant difference at $p < 0.05$.

3. Results and discussion

3.1. Inhibitory effect of morin on α-glucosidase in vitro

As shown in Fig. 1A, morin exhibited expected inhibition on α-glucosidase in a dose-dependent manner. With increasing amounts of morin, the activity of α-glucosidase decreased rapidly until completely inhibited. The concentrations of morin and acarbose that resulted in a loss of 50% enzyme activity (IC_{50}) were determined to be (4.48 ± 0.04) μM and (402 ± 5) μM, respectively. These results indicated that morin was a powerful α-glucosidase inhibitor in vitro compared with acarbose. The IC_{50} value of morin on α-glucosidase was lower than that of the

previous report (40.0 μM),[18] which may be due to the difference in the source of enzyme, the manufacturer of drugs as well as the conditions of measurement. Previous studies found that luteolin and kaempferol with a similar structure to morin exhibited inhibition of α-glucosidase with IC_{50} values of 172 and 11.6 μM, respectively.[25,26] Compared to luteolin and kaempferol, morin inhibited α-glucosidase more effectively. This might be because the 3-hydroxyl groups on C ring of morin played an important role in the inhibition and the hydroxylations at the 3 positions of flavones enhanced the inhibitory activity. It was reported that the hydrogen atoms of the hydroxyl groups at positions 3 and 5 of the flavones formed intramolecular hydrogen bonds with the oxygen atom of the carbonyl which favored the molecule planarity and delocalized the π electrons.[27] The inhibition of kaempferol on α-glucosidase was weaker than morin which was likely due to the lack of hydroxyl groups at the position of 2' on B ring. These results were in line with that of a previous report that the inhibitory activity on α-glucosidase increased considerably with an increase in the number of hydroxyl group on B ring and the hydroxylation at the 3 position enhanced the inhibitory effect as well.[28]

In order to determine the reversibility of morin mediated inhibition, the plots of reaction rate *vs.* [α-glucosidase] at different morin concentrations were constructed (Fig. 1B). All the lines were linear and passed through the origin, and the slope decreased with the increase of morin concentration. The results implied that the amount of efficient enzyme available didn't decrease in the presence of morin, but it did lead to the inhibition of α-glucosidase and an overall decrease of enzyme activity as regards the oxidation of *p*NPG. These results confirmed the reversibility of morin on α-glucosidase inhibition and a noncovalent intermolecular interaction between morin and α-glucosidase.[22]

3.2. Anti-glycation activity of morin

The results showed that morin effectively inhibited the generation of AGEs in the BSA/fructose system (Fig. 2A) in a dose−dependent manner. Morin at 100 and 200 μM inhibited the formation of AGEs by 59% and 81%, respectively, which was more effective than that of AG at the same concentration (14% and 21%). The inhibition rates of AG at 1.0 and 2.0 mM were 77% and 90%, respectively. As shown in Fig. 2B and C, the fluorescence intensity of glycated albumins was higher than that of non−glycated, indicating the formation of glycation products. Furthermore, the fluorescence intensity decreased as the increase in the concentrations of both morin and AG with visible red shifts of the maximum λ_{em} from 453 to 475 nm and from 453 to 460 nm, suggesting the increase of polarity of the fluorophores microenvironments.[3] Morin was found to inhibit the activity of α-glucosidase and attenuate the generation of AGEs *in vitro*, which suggested that morin is a potential antidiabetic compound for prevention of hyperglycemia induced damage. It was reported that dietary flavonoids such as quercetin, kaempferol and luteolin could inhibit the generation of AGEs,[29] so both kaempferol and luteolin have the same property as morin toward preventing the damage induced by hyperglycemia. These results suggested foods rich in flavonoids or supplements may delay the development of DM2 which was coincident with the previous reports.[7] However, it is worth noting that Lavelli and coworkers reported that when white grape skin rich in flavonoids as a food ingredient was added to tomato pruee and wheat flat bread, the experimental increased percentages of inhibition on α-glucosidase and α-amylase were lower than the expected increase, the results are most probably due to the binding of the higher mass proanthocyanidins of grape skin to the food matrix,[30] thus decreasing or losing their efficacy.

3.3. Kinetic mode of inhibition of morin on α-glucosidase

Lineweaver−Burk plots were employed to investigate the inhibition kinetics of morin to α-glucosidase. The double reciprocal plots generated a series of lines which intersect one another in the second quadrant with different slopes and intercepts (Fig. 1C). Furthermore, the apparent K_m and V_{max} changed simultaneously, and the value of V_{max} decreased as K_m increased. The results indicated that morin caused a mixed−type inhibition, which meant the morin could bind to both the free enzyme and the enzyme−substrate complex.[22] The secondary replot of Slope or Y-intercept *vs.* [morin] was linear (Fig. 1C), suggesting that morin had a single inhibition site or a single class of inhibition sites on α-glucosidase. Based on Eqs. (2) and (3), the values of K_i and K_{is} were obtained to be (1.68 ± 0.3) μM and (2.90 ± 0.4) μM, respectively. The value of K_{is} was obviously greater than that of K_i, indicating that the affinity of inhibitor to free enzyme may be stronger than that of enzyme−substrate complex.[31] The inhibitory mode of kaempferol and luteolin towards α-glucosidase was a mix-type and noncompetitive. The values of K_i for luteolin and kaempferol were 1.40×10^{-4} and 1.31×10^{-5} L mol^{-1}, respectively. The increasing order of the K_i was morin < kaempferol < luteolin, indicating that the α-glucosidase inhibition effect of morin was supposed to be the maximum while that of luteolin to be the minimum, which might be due to the differences in affinity to the enzyme inhibition sites. The inhibition ability of the three flavonoids to α-glucosidase infered from the values of K_i was consistent with that of experimental results.[32]

3.4. Inactivation kinetics and rate constants

To determine inactivation kinetics and rate constants, the time courses of α-glucosidase inhibition at different concentrations of morin were conducted (Fig. 1D). For the various concentrations of morin, the catalytic activities of α-glucosidase

were decreased rapidly from 0 to 3000 s, and then the activity stabilized as the time increased. The subsequent analysis based on semi−logarithmic plots (Fig. 1D) suggested that the processes were monophasic in the time range of detectable activity changes.[22] All the processes followed first−order kinetics. The inactivation rate constants and transition free−energy change ($\Delta\Delta G°$) that might be induced by the inactivation of α-glucosidase caused by morin (Table 1).

3.5. Fluorescence quenching of α-glucosidase by morin

The fluorescence spectroscopy was used to investigate the binding between morin and α-glucosidase. As shown in Fig. 2D, α-glucosidase presented a strong emission peak at 343 nm, but the supposed emission wavelength of tyrosine (Tyr) at 304−310 nm disappeared because it was nearly quenched by tryptophan (Trp) on account of the efficient energy transfer from Tyr to Trp, i.e. the internal quenching effect.[33] In addition, morin didn't exhibit fluorescence at 343 nm under the same experiment conditions. The fluorescence intensity of α-glucosidase decreased dramatically with the increase of morin concentration, while the shift in the position of emission peak was not detected. The phenomenon would be a direct evidence for the interaction between morin and α-glucosidase.

Fluorescence quenching may result from a variety of processes, including dynamic quenching, static quenching and a combination of them. Dynamic quenching was caused by the collision between the fluorophore and quencher, while static quenching was a formation of the ground−state complex.[33] Their different dependence on the temperature and excited life−time can be used to distinguish these two mechanisms. The mechanism of the ligand binding to α-glucosidase was probed by using Stern−Volmer equation:[23]

$$\frac{F_0}{F} = 1 + K_{SV}[Q] = 1 + K_q \tau_0 [Q] \quad (5)$$

where F_0 and F are the fluorescence intensities in the absence and presence of morin, respectively. [Q] represents the concentration of morin. K_{SV} is the Stern−Volmer quenching constant, which could be calculated by linear regression of a plot of F_0/F against [Q]. K_q is the biomolecule quenching rate constant ($K_q = K_{SV}/\tau_0$), τ_0 is the average lifetime of fluorophore in the absence of quencher (the value is 10^{-8} s).[25]

The values of K_{SV} from the plot F_0/F versus [Q] (the inset in Fig. 2D) at three different temperatures (292, 298 and 310 K) are listed in Table 2. All the three lines showed high linearity, suggesting that the quenching process could be only one type, either dynamic or static quenching, a combination of these may be excluded. The values of K_{SV} decreased with the increase of temperature, and the K_q values at three temperatures (292, 298, and 310 K) were 6.45×10^{12}, 5.73×10^{12}, 5.29×10^{12} L $mol^{-1}s^{-1}$, respectively, which were two orders of magnitude greater than the maximum scatter collision quenching constant of the biomolecule (2.0×10^{10} L $mol^{-1}s^{-1}$).[34] These results indicated that the quenching of α-glucosidase by morin was a static quenching process rather than a dynamic collision quenching.

3.6. Binding constant and number of binding sites

For static quenching, an improved method was used to calculate the binding constant (K_a) and the number of binging sites (n)[26]

$$\log\frac{F_0 - F}{F} = n\log K_a - n\log\frac{1}{[Q_t] - \frac{(F_0 - F)[P_t]}{F_0}} \quad (6)$$

F_0 and F are the same with equation (5); $[P_t]$ and $[Q_t]$ mean the total concentrations of the enzyme and morin, respectively. The values of K_a and n were calculated from the slope and intercept of the plots of $\log(F_0-F)/F$ versus $\log([Q_t]-[P_t]\ (F_0-F)/F)$, and the results were summarized in Table 2. The values of n were approximately equal to 1, indicating only one binding site for morin on α-glucosidase, which was in accordance

with the result of Lineweaver-Burk plot analysis. The K_a value at 298K was 5.58 × 10^4 L mol^{-1}, suggesting that a higher affinity existed between morin and α-glucosidase, and the decreasing trend of K_a along with the increase of temperature indicated the stability of the morin−α-glucosidase complex decreased at higher temperature. The result also further proved that the fluorescence quenching was a static quenching process.[33]

3.7. Thermodynamic analysis and binding forces

In order to further characterize the intermolecular forces between α-glucosidase and morin, the thermodynamic parameters were estimated. There are four main types of non−covalent interactions between ligand and macromolecule, i.e., electrostatic interactions, multiple hydrogen bonds, van der Waals interactions and hydrophobic forces. If the temperature does not vary drastically, the enthalpy change ($\Delta H°$) can be regarded as a constant, and then its value and the value of entropy change ($\Delta S°$) can be calculated from the Van't Hoff equation:

$$\log K_a = -\frac{\Delta H°}{2.303RT} + \frac{\Delta S°}{2.303R} \quad (7)$$

The free energy change ($\Delta G°$) can be determined from the following equation:

$$\Delta G° = \Delta H° - T\Delta S° \quad (8)$$

where K_a is the binding constant at the corresponding temperature (T), T represents the absolute temperature used in the experiment and R is the gas constant (8.314 J $mol^{-1}K^{-1}$). The plot between $\log K_a$ and $1/T$ showed a good linearity, from which the values of $\Delta H°$ and $\Delta S°$ were obtained (Table 2). The negative value of $\Delta G°$ suggested that the binding process between morin and α-glucosidase occurred spontaneously. The conclusion that the reaction was an exothermic process deducing from the negative value of $\Delta H°$ (−7.22 kJ mol^{-1}) was consistent with that of the decreasing

tendency of K_a with temperature.[35] Besides, the positive value of $\Delta S°$ (65.25 J $mol^{-1}K^{-1}$) was frequently taken as a typical evidence for hydrophobic interaction and the negative value of $\Delta H°$ indicated the existence of hydrogen bond.[32] According to the theory of Ross and Subramanian,[36] $\Delta H°<0$ and $\Delta S°>0$ indicated that hydrophobic forces and hydrogen bonding exerted a predominant role in the interaction between morin and α-glucosidase.

3.8. Binding distance

The quantum yield of α-glucosidase was calculated by comparing fluorescence intensity of α-glucosidase and human serum albumin (HSA, as a standard solution,quantum yield 0.13) under the same condition. The following equation was used to determine the quantum yield:[37]

$$\varphi_x = \varphi_{st} \cdot \frac{F_x}{F_{st}} \cdot \frac{A_{st}}{A_x} \quad (9)$$

where F_{st} and F_x represent the fluorescence intensities of HSA and α-glucosidase; A_{st} and A_x indicate the absorbence of HSA and α-glucosidase at excitation wavelength of HSA; φ_{st} and φ_x are the fluorescence quantum yields of HSA and α-glucosidase, respectively. φ_x was calculated to be 0.084 based on equation (9). According to Förster non−radiative energy transfer theory, the distance r between the donor and acceptor can be calculated by the following equations: [37]

$$E = \frac{F_0 - F}{F_0} = \frac{R_0^6}{R_0^6 + r^6} \quad (10)$$

$$R_0^6 = 8.79 \times 10^{-25} \kappa^2 N^{-4} \varphi J \quad (11)$$

$$J = \frac{\Sigma F(\lambda) \varepsilon(\lambda) \lambda^4 \Delta\lambda}{\Sigma F(\lambda) \Delta\lambda} \quad (12)$$

here E is the energy transfer efficiency between the donor and the acceptor; R_0 means

Förster distance or critical distance when the energy transfer is 50%; F and F_0 are the fluorescence intensities of α-glucosidase in the presence and absence of morin; κ^2 is the spatial orientation factor of the dipole and $\kappa^2 = 2/3$ for random orientation as in fluid solution; N represents the refraction index of the medium ($N = 1.336$); φ is the fluorescence quantum yield of α-glucosidase ($\varphi = \varphi_x = 0.084$); J is the overlap integral of the fluorescence emission spectrum of the donor and the absorption spectrum of the acceptor, and can be calculated by equation(12); $F(\lambda)$ is the fluorescence intensity of the donor at wavelength λ; $\varepsilon(\lambda)$ is the extinction coefficient of the acceptor at λ. The overlap of the fluorescence emission spectrum of α-glucosidase and the absorption spectrum of morin which had the same concentration as α-glucosidase was shown in Fig. 2E. Base on equations (10)−(12), $J = 1.55 \times 10^{-14}$ cm^3 L mol^{-1}, $R_0 = 2.49$ nm, $r = 2.52$ nm, obviously, the distance between the donor and acceptor r was less than 8 nm, and $0.5R_0 < r < 1.5R_0$, suggesting that the fluorescence quenching of α-glucosidase by morin was the static procedure combining with a non-radiative energy transfer process.[37]

3.9. Conformational changes

The effect of morin on the Tyr and Trp and change in their fluorescence emission bands were monitored by synchronous fluorescence spectroscopy. As shown in Fig. 3A and B, the fluorescence intensities of both Tyr and Trp decreased regularly when the concentration of morin increased, but their maximum emission wavelength did not shift obviously, indicating that the polarity and hydrophobicity around Trp and Tyr residues were not significantly affected by morin.[38]

"Phase diagram" method of fluorescence was firstly established by Burstein in 1971, which was used to analyze the fluorescence data of protein molecules, based on the intrinsic fluorescence emission intensity of protein molecules at a fixed emission

wavelength.[39] The phase diagram of fluorescence was obtained by measuring the fluorescence emission intensities $I(\lambda_1)$ and $I(\lambda_2)$ with different concentrations of morin at two specific emission wavelengths λ_1 and λ_2. The following relationships exist between these two variables:[40]

$$I(\lambda_1) = \mathrm{a} + bI(\lambda_2) \quad (13)$$

$$a = I_1(\lambda_1) - \frac{I_2(\lambda_1) - I_1(\lambda_1)}{I_2(\lambda_2) - I_1(\lambda_2)} I_1(\lambda_2) \quad (14)$$

$$b = \frac{I_2(\lambda_1) - I_1(\lambda_1)}{I_2(\lambda_2) - I_1(\lambda_2)} \quad (15)$$

The linearity of $I(\lambda_1)$ and $I(\lambda_2)$ in the relationship of equation (13) indicates that the changes of protein environment induced an all-or-none transition between two different conformations, suggesting that no partial intermediates exist. What's more, the nonlinearity suggests the sequential character of structural transformations. In addition, every linear portion of the plot depicts an individual all-or-none transition, which means there may be one or more folding intermediate states in the conformational change process of protein.[40] Here λ_1 (320 nm) and λ_2 (360 nm) were chosen on both sides of the maximum emission wavelength, so the phase diagram of fluorescence would be more accurate. The phase diagram of fluorescence of α-glucosidase containing different concentrations of morin was shown in Fig. 3C. The good linearity indicated an all-or-none transition without intermediates in the conformational change process of α-glucosidase induced by morin. The result was concordant with that from the inactivation kinetics investigation.

In order to further monitor the conformational change of α-glucosidase induced by morin, CD spectra of far and near−UV region were employed to analyze the binding of small ligand to chiral macromolecules. The far−UV region (190−250 nm) can be used to investigate the secondary structure contents of proteins, in which the main

absorbing groups are peptide bonds. As shown in Fig. 3D, the far−UV CD spectra of α-glucosidase were characterized primarily by two negative bands at 210 and 222 nm, which are characteristics of the helical structure and resulted from the $n \rightarrow \pi^*$ and $\pi \rightarrow \pi^*$ electron transfer for the peptides bonds of the α-helix.[41] Along with the addition of morin to the α-glucosidase, a decrease in CD intensities of α-glucosidase at both two bands (shifting to zero levels) were observed, suggesting that the interaction between morin and α-glucosidase led to the conformational changes of the enzyme. The contents of different secondary structures of α-glucosidase was analyzed. Compared with the free α-glucosidase, the contents of α-helix and β-Turn tended to decline (from 30.1% to 25.4% and from 19.0 to 17.2%, respectively) at the molar ratio of morin to α-glucosidase of 6:1, while the contents of β-sheet and random coil tended to increase (from 27.1% to 31.2% and from 23.8% to 26.2%, respectively). The decrease in α-helix and increase in random coil indicated that the binding of morin to α-glucosidase induced the unfolding of protein structure and a decline in its stability, which resulted in the decrease of the α-glucosidase catalytic activity.[42]

The effect of morin on the tertiary structure of α-glucosidase was investigated by near−UV CD spectra. Aromatic amino acid residues in proteins, such as Trp, Tyr, Phe, and disulfide bonds in the asymmetric microenvironment show CD signals in the near−UV region (250−350 nm) while morin is achiral molecule without CD signals. Every aromatic amino acid has a characteristic wavelength, 250−270 nm represent Phe, 270−290 nm is the characteristic wavelength of Tyr, while Trp contributes in the range from 270 to 290 nm.[43] As shown in Fig. 3E, near−UV CD spectra of α-glucosidase in the absence and presence of morin exhibited a broad positive band with a maximum at 297 nm. With the increase of morin concentration, the intensity slightly aggrandized without a shift of the maximum peak position, and the sharp of

spectra did not significantly change. The phenomenon might indicate an alteration of the asymmetric microenvironment at the Trp residues. The increase of signal may suggest the weakening of flexibility of Trp residues.[44,45] The near−UV CD spectra of α-glucosidase was similar to the previous report with a mild difference in the position of maximum peak.[46]

3.10. Computational docking analysis

Molecular docking, a complementary application, has recently been widely employed to further substantiate the drug−protein interaction. The AutoDock strategy is applied to search the entire surface of protein for binding sites and simultaneously optimize the conformations of the peptides. The structure of α-glucosidase was determined through the homology modeling (PDB ID: 3A4A; gi number 411229). A cluster with the lowest energy (−4.35 kcal mol^{-1}) and most frequent locus (46 out of 100, the red bar in Fig. 4A) from 100 docking runs was chosen as the most optimal cluster for binding orientation analysis. The predicted binding energy was a little bit higher than $\Delta G°$ (−6.49 kcal mol^{-1}) acquired from the thermodynamic analysis at 298 K which might be due to the lack of desolvation energy since the molecular docking was carried out under simulation of vacuum environment.[25]

As shown in Fig. 4B, the competitive inhibitor acarbose bound in the catalytic active cavity which was surrounded by the amino acid residues i.e. Phe178, Asp69, Val410, Glu411, Phe314, Pro312, His351, Asp352, Glu277 and Val216 in α-glucosidase, these residues were reported to play pivotal roles in the catalytic mechanism.[25,26] It was found that the binding site for morin was close to the active site cavity, and it was surrounded by the residues Ser304, Asp307, Thr310, Gly309, Pro320, Phe321, Asp325, Trp326, Ala329 and Glu332 (Fig. 4C). Furthermore, three hydrogen bonds were formed between morin and the residues of α-glucosidase. The

first one was established between the hydrogen of hydroxyl group at C−4' position on B ring of morin and Glu332 with a distance of 2.202Å, the second one between the hydrogen of hydroxyl group at C−3 on C ring of morin and Ser304 (1.955Å), and the third one between the hydrogen of hydroxyl group at C−7 on A ring of morin and Pro320 (1.974 Å). This result indicated hydrogen bond was another main role in the binding of morin to α-glucosidase, which confirmed the result of thermodynamic analysis. The formation of hydrogen bond between the hydroxyl group at C−3 and C−4' of morin and the residues might explain why morin exhibited higher inhibition potency toward α-glucosidase compared to luteolin and kaempferol. The morin was not totally inserting into the hydrophobic cavity but close to the pocket of active site, suggesting that hydrophobic interactions were exist. The binding of morin to α-glucosidase inhibited the enzyme activity, which might be because morin induced the conformational changes of α-glucosidase and led to the cleft closure to avoid the entrance of substrate. Predicting the binding site on α-glucosidase by the molecular docking provided supportive data for morin−induced inhibition, and the results suggested that morin actually interacted with the amino acid residues around the activity site which was consistent with a previous report.[25]

4. Conclusions

The inhibitory mechanism of morin on α-glucosidase activity was investigated by multispetroscopic methods and molecular simulations. The principal results of this study were summarized as the following: (i) morin inhibited the catalytic activity of α-glucosidase in a mixed−type manner, and it was also able to inhibit the formation of AGEs in a dose-dependent manner. (ii) the fluorescence quenching of α-glucosidase was due to the formation of a morin−enzyme complex in a static procedure which was mainly driven by hydrophobic forces and hydrogen bonding. (iii) the binding of morin

513 to α-glucosidase induced rearrangement and conformational changes of the enzyme.
514 (iv) the binding site on α-glucosidase for morin was not the same as the competitive
515 inhibitor acarbose. These results suggested that morin could be a promising
516 α-glucosidase inhibitor that deserves further investigations including the binding of
517 morin to the food matrix, and the ingestion of morin−rich foods may have a positive
518 effect for prevention of hyperglycemia induced damage.

519 ## Acknowledgments

520 This work was financially supported by the National Natural Science Foundation of
521 China (Nos. 31460422 and 31060210), the Natural Science Foundation of Jiangxi
522 Province (20143ACB20006), the Foundation of Jiangxi Provincial Office of
523 Education (GJJ150187), the Objective-Oriented Project of State Key Laboratory of
524 Food Science and Technology (SKLF-ZZA-201612), and the Nanchang University
525 Postgraduate Innovation Fund (CX2015112).

526 ## References

527 1 S. Ghosh, P. More, A. Derle, A. B. Patil, P. Markad, A. Asok and D. D. Dhavale,
528 *PloS one*, 2014, **9**, e106039.
529 2 M. D.Gunawan-Puteri and J. Kawabata, *Food Chem.,* 2010, **123***,* 384–389.
530 3 A. Szkudlarek, A. Sulkowska, M. Maciqzek-Jurczyk, M. Chudzik and J.
531 Równicka-Zubik, *Spectrochim. Acta, Part A.,* 2016, **152**, 645–653.
532 4 Z.Yu, Y. Yin, W. Zhao, Y. Yu, B. Liu, J. Liu and F. Chen, *Food Chem.,* 2011**, 129**,
533 1376–1382.
534 5 S. Adisakwattana, P. Jiphimai, P. Prutanopajai, B. Chanathong, S. Sapwarobol
535 and T. Ariyapitipan, *Int. J. Food Sci. Nutr.,* 2010, **61,** 295–305.
536 6 Y. T. Deng, S. Y. Lin-Shiau, L. F. Shyur and J. K. Lin, *Food Funct.,* 2015, **6,**

1539–1546.

7 G. Williamson, Mol. Nutr. Food Res., 2013, 57, 48–57.

8 F. Rahim, F. Malik, H. Ullah, A. Wadood, F. Khan, M. T. Javid and K. M. Khan, *Bioorg. Chem.,* 2015, **60,** 42–48.

9 T. T. Chai, M. T. Kwek, H. C. Ong and F. C. Wong, *Food Chem.,* 2015, **186,** 26–31.

10 S. Pashikanti, D. R. de Alba, G. A. Boissonneault and D. Cervantes-Laurean, *Free Radical Biol. Med.,* 2010, **48,** 656–663.

11 D. F. Pereira, L. H. Cazarolli, C. Lavado, V. Mengatto, M. S. R. B. Figueiredo, A. Guedes and F. R. M. B. Silva, *Nutr.,* 2011, **27,** 1161–1167.

12 A. M. Mendoza-Wilson, H. Santacruz-Ortega and R. R. Balandrán-Quintana, *J. Mol. Struct.,* 2011, **995,** 134–141.

13 Y. Yoshie-Stark, H. Ya-Pei and S. Takeshi, *J. Tokyo Univ. Fish.*, 2003, **89**, 1–6.

14 S. Cox, N. Abu-Ghannam and S. Gupta, *Int. Food Res. J.*, 2010, **17**, 205–220.

15 M. Marotti and R. Piccaglia, *J. Food Sci.*, 2002, **67**, 1229–1232.

16 W. Thuaytong and P. Anprung, *Food Sci. Technol. Int.*, 2011, **17**, 205–212.

17 H. L. Yue, Y. J. Hu, H. G. Huang, S. Jiang and B. Tu, *Spectrochim. Acta, Part A.,* 2014, **130,** 402–410.

18 M. Iio, A. Yoshioka, Y. Imayoshi, C. Koriyama and M. Ayako, *Agric. Biol. Chem.,* 1984, **48,** 1559–1563.

19 T. Ohta, S. Sasaki, T. Oohori, S. Yoshikawa and H. Kurihara, *Biosci. Biotechnol. Biochem.,* 2002, **66,** 1552–1554.

20 S. H. Wang, J. C. Chang, R. Pokkaew, J. F. Lee and R. Y. Y. Chiou, *J. Agric. Food Chem.,* 2011, **59,** 6906–6912.

21 Y. X. Si, S. Ji, N. Y. Fang, W. Wang, J. M. Yang, G. Y. Qian and S. J. Yin, *Process*

Biochem., 2013, **48,** 1706–1714.

22 Z. J. Wang, J. Lee, Y. X. Si, S. Oh, J. M. Yang, D. Shen and S. J. Yin, *Process Biochem.,* 2013, **48,** 260–266.

23 X. Peng, X. Wang, W. Qi, R. Huang, R. Su and Z. He, *Food Funct.,* 2015, **6,** 2712–2726.

24 S. Escandón-Rivera, M. González-Andrade, R. Bye, E. Linares, A. Navarrete and R. Mata, *J. Nat. Prod.,* 2012, **75,** 968–974.

25 J. Yan, G. Zhang, J. Pan and Y. Wang, *Int. J. Biol. Macromol.,* 2014, **64,** 213–223.

26 X. Peng, G. Zhang, Y. Liao and D. Gong, *Food Chem.,* 2015, **190,** 207–215.

27 A. M. Ponce, S. E. Blanco, A. S. Molina, R. García-Domenech and J. Gálvez, *J. Chem. Inf. Comput. Sci.,* 2000, **40,** 1039–1045.

28 K. Tadera, Y. Minami, K. Takamatsu and T. Matsuoka, *J. Nutr. Sci. Vitaminol.,* 2006, **52,** 149–153.

29 L. Liu, Y. Xie, Z. Song, S. Shang and X. Chen, *Mol. BioSyst.,* 2012, **8,** 2183–2187.

30 V. Lavelli, P. S. Harsha, P. Ferranti, A. Scarafoni and S. Iametti, *Food Funct.*, 2016, **7**, 1655–1663.

31 J. P. Zhang, Q. X. Chen, K. K. Song and J. J. Xie, *Food Chem.,* 2006, **95,** 579–584.

32 C. Tang, , L. Zhu, Y. Chen, R. Qin, Z. Mei, J. Xu and G. Yang, *RSC Adv.,* 2014, **4,** 10862–10874.

33 S. Bi, B. Pang, T. Wang, T. Zhao and W. Yu, *Spectrochim. Acta, Part A.,* 2014, **120,** 456–461.

34 Y. Xie, W. Yang, X. Chen and J. Xiao, *Food Funct.,* 2014, **5,** 2582–2589.

35 A. Basu, and G. S. Kumar, *Food Funct.,* 2014, **5,** 1949–1955.

36 P. D. Ross and S. Subramanian, *Biochemistry.,* 1981, **20,** 3096–3102.

37 S. Bi, L. Yan, Y. Wang, B. Pang and T. Wang, *J. Lumin.,* 2012, **132,** 2355–2360.

38 M. Maciążek-Jurczyk, A. Sułkowska and J. Równicka-Zubik, *Spectrochim. Acta, Part A.* 2015, **152,** 537–550.

39 I. M. Kuznetsova, K. K. Turoverov and V. N. Uversky, *J. Proteome Res.,* 2004, **3,** 485–494.

40 X. Ji, X. Ma and L. Bian, *Chem. Res. Chin. Univ.,* 2014, **30,** 222–227.

41 Y. J. Wang, G. W. Zhang, J. K. Yan and D. M. Gong, *Food Chem.,* 2014, **163,** 226–233.

42 Y. J. Wang, G. W. Zhang, J. H. Pan and D. M. Gong, *J. Agric. Food Chem.,* 2015, **63,** 526–534.

43 J. Zhang, L. Xiao, Y. Yang, Z. Wang and G. Li, *Food Chem.,* 2014, **149,** 99–106.

44 N. Tanaka, S. Kajimoto, D. Mitani and S. Kunugi, *Biochim. Biophys. Acta, Protein Struct. Mol. Enzymol.,* 2002, **1596,** 318–325.

45 H. R. Karbalaei-Heidari, A. E. Habibi, K. Khajeh, B. Ranjbar and M. Nemat-Gorgani, *Appl. Biochem. Biotechnol.,* 2004, **117,** 123–132.

46 C. Raasch, M. Armbrecht, W. Streit, B. Höcker, N. Sträter and W. Liebl, *FEBS Lett.,* 2002, **517,** 267–271.

607 **Figureure captions**

608 **Fig. 1.** (A)Inhibitory effects of morin and acarbose on α-glucosidase (pH 6.8, T = 310
609 K). (B) plots of *v* versus [α-glucosidase]. *c*(*p*NPG) = 454μM, *c*(morin) = 0, 1.5, 3.5,
610 5.0, and 7.5 μM for curve a→e, respectively. (C) Lineweaver−Burk plots.
611 *c*[α-glucosidase] = 50.8 nM, and *c*(morin) = 0, 1.5, 3.5 and 5.0 μM for curve a→d,
612 respectively. The secondary plots of slope (the upper left) and Y−intercept (the lower
613 left) *vs*. [morin] were in the inset. (D)Kinetic time-courses for relative activity of
614 α-glucosidase in the presence of morin at 1.50, 2.25, 3.00, 4.50, 6.00 μM for curve
615 a→e, respectively. Semi-logarithmic plots analysis for morin at 1.5 (the upper right)
616 and 4.5 μM (the lower right). *c*(α-glu) = 50.8 nM, *c*(*p*NPG) = 454 μM.

617 **Fig. 2.** (A) Inhibitory activity of morin and AG on the formation of AGEs (pH 7.4, *T* =
618 50 ºC). (B) Fluorescence spectra of the AGEs in the absence or presence of morin. (C)
619 Fluorescence spectra of the AGEs in the absence or presence of AG. The red solid line
620 means the emission spectrum of BSA without fructose at the same conditions. (D)
621 Fluorescence spectra of α-glucosidase in the presence of morin at various
622 concentrations (pH 6.8, *T* = 298 K), *c*[α-glucosidase] = 1.0 μM and *c*(morin) = 0, 2.0,
623 4.0, 5.9, 7.9, 9.8, 11.7, 13.6, 15.5, 17.4, 19.2 and 21.1 μM for curves a→l, respectively.
624 Curve m shows the emission spectrum of morin at the concentration of 2.0 μM. The
625 Stern–Volmer plots for the fluorescence quenching of α-glucosidase by morin at
626 different temperatures were inserted. (E) Spectral overlaps of the fluorescence
627 spectrum of α-glucosidase (a) with the absorption spectrum of morin (b).
628 *c*(α-glucosidase) = *c*(morin) = 1.0 μM.

629 **Fig. 3.** (A) Synchronous fluorescence spectra of α-glucosidase in the absence and
630 presence of morin (pH 6.8, *T* = 298 K). Δλ = 15 nm. (B) Δλ = 60 nm. *c*(α-glucosidase)
631 = 1.0 μM. *c*(morin)=0, 2.0, 4.0, 5.9, 7.9, 9.8, 11.7, 13.6, 15.5, 17.4, 19.2 and 21.1 μM

for curves a→l, respectively. (C) The phase diagram of fluorescence of α-glucosidase with different concentrations of morin (pH 6.8, T = 298 K). c(α-glucosidase) = 1.0 μM. c(morin)=0, 2.0, 4.0, 5.9, 7.9, 9.8, 11.7, 13.6, 15.5, 17.4, 19.2 and 21.1 μM. (D) The far–UV CD spectra of α-glucosidase with increasing amounts of morin. The molar ratios of morin to α-glucosidase were 0:1, 4:1 and 6:1 for curves a→c, respectively. (E) The near–UV CD spectra of α-glucosidase with increasing amounts of morin. The molar ratios of α-glucosidase to morin were 1:0, 1:2, 1:4 and 1:6 for curves a→d, respectively.

Fig. 4. (A) Cluster analyses of the AutoDock docking runs of morin with α-glucosidase. (B) Predicted binding mode of morin docked with α-glucosidase on molecular surface. The green areas represent the catalytic activity site of α-glucosidase. (C) The interaction between morin and α-glucosidase. The pink stick structure was used to represent the morin while the green stick denotes the residues of α-glucosidase. The short solid green line stands for hydrogen bonds.

Table 1. Inactivation rate constants of α-glucosidase in the presence of morin.

Morin($\times 10^{-6}$mol L^{-1})	Inactivation rate constants($\times 10^{-4}s^{-1}$)[a]	Transition free-energy change (kJ mol^{-1} s^{-1})[b]
	k	
1.50	2.64	21.24
2.25	3.19	20.75
3.00	2.95	21.02
4.50	4.31	19.97
6.00	5.01	19.58

[a] Data were calculated as shown in Figureure 1C; *k* is the first–order rate constant.

[b] Transition free–energy change per s. is $\Delta\Delta G^{\circ} = -RT\ln k$, where k is a time constant of the inactivation reaction.

Table 2. The quenching constants K_{SV}, binding constants K_a, number of binding sites n and relative thermodynamic parameters of the interaction between morin and α-glucosidase at different temperatures.

T(K)	K_{SV} ($\times 10^4$L mol^{-1})	R^a	K_a ($\times 10^4$L mol^{-1})	n	R^b	$\Delta H°$ (kJ mol^{-1})	$\Delta G°$ (kJ mol^{-1})	$\Delta S°$ (J mol^{-1}K^{-1})
292	6.45 ± 0.04	0.9980	6.26 ± 0.04	1.04 ± 0.01	0.9984		–26.77±0.3	
298	5.73 ± 0.03	0.9984	5.58 ± 0.02	1.16 ± 0.03	0.9998	–7.72 ± 0.2	–27.16±0.2	65.25 ± 0.1
310	5.29 ± 0.03	0.9986	5.16 ± 0.01	1.19 ± 0.02	0.9997		–27.94±0.2	

[a] R is the correlation coefficient for the K_{SV} values.

[b] R is the correlation coefficient for the K_a values.

Fig. 1.

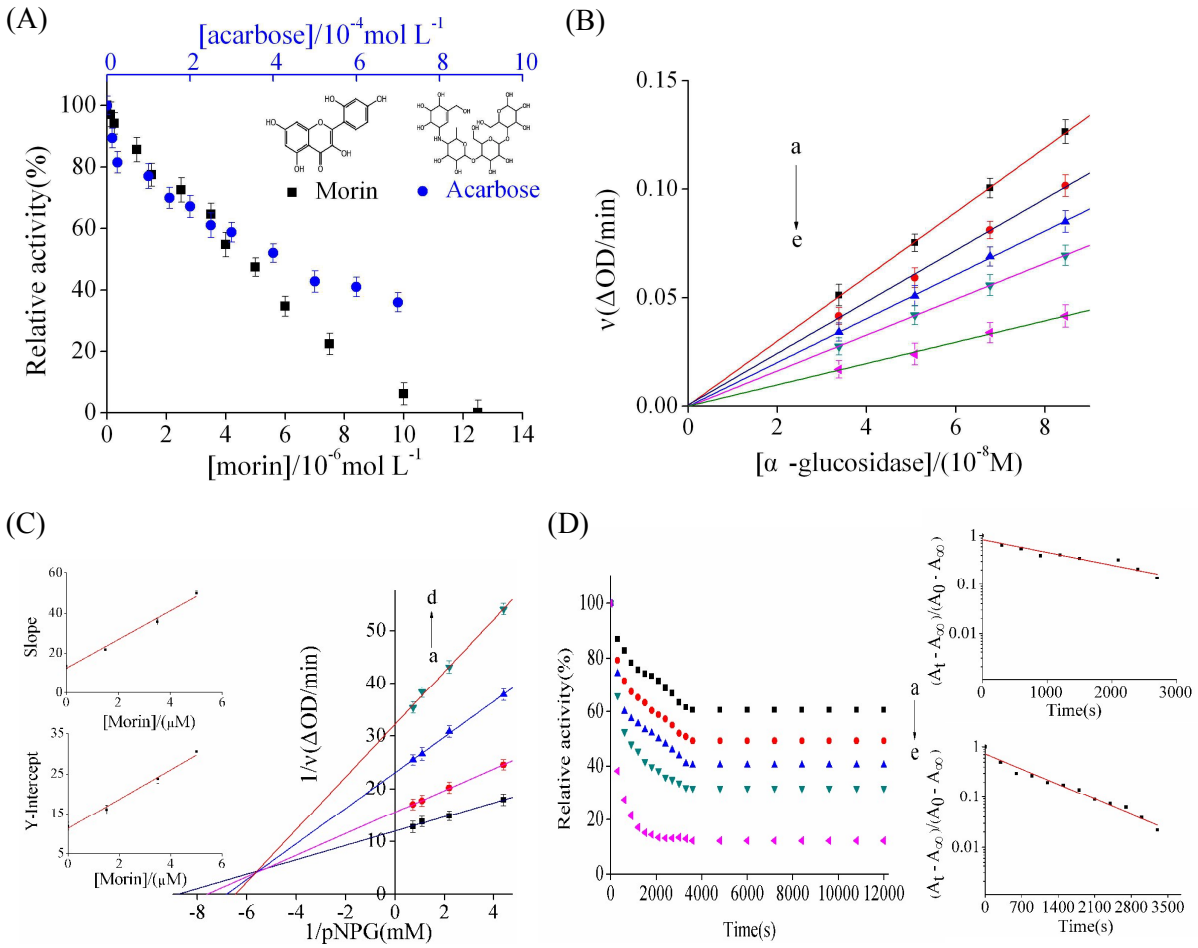

Fig. 2.

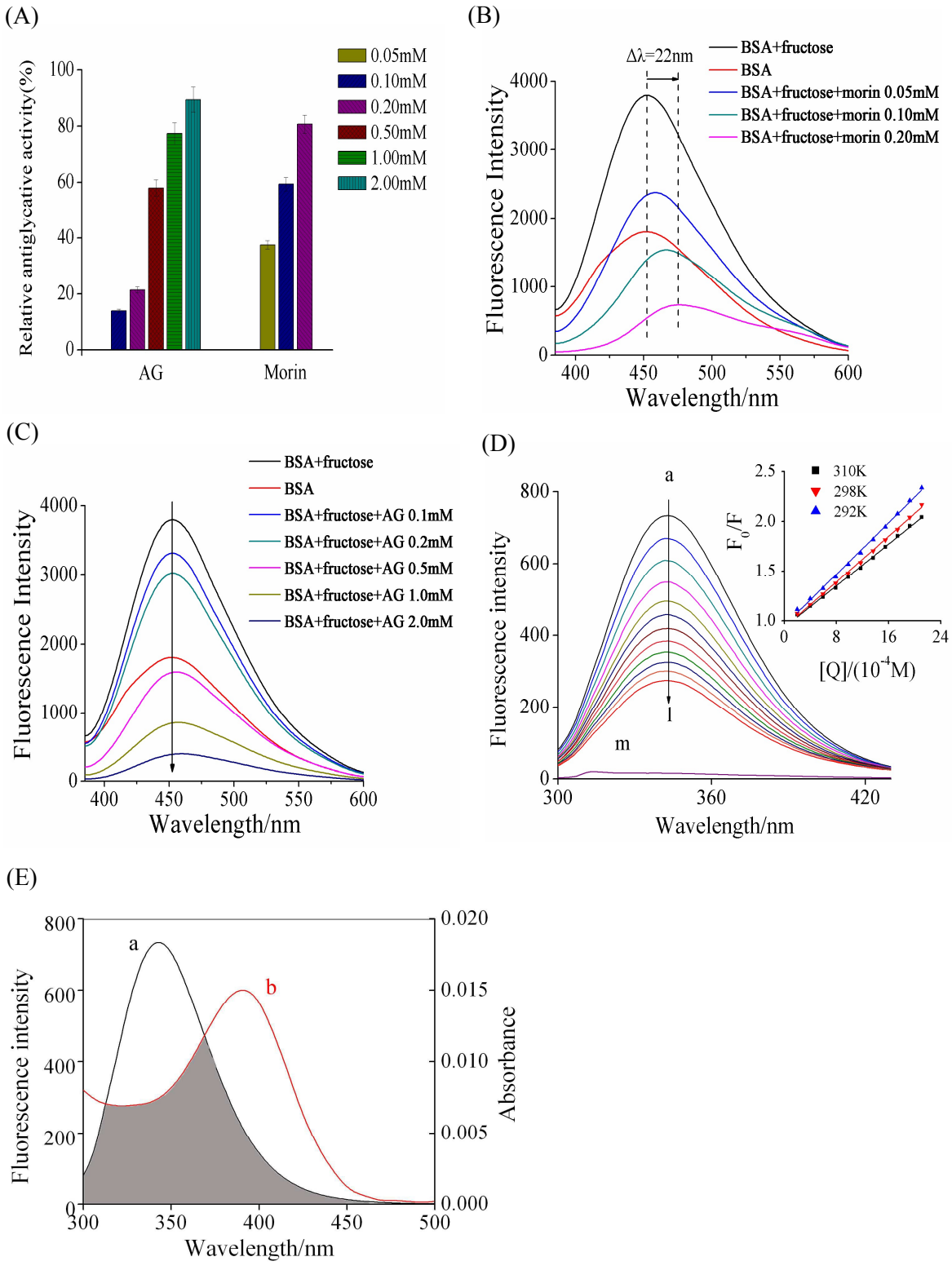

Fig. 3.

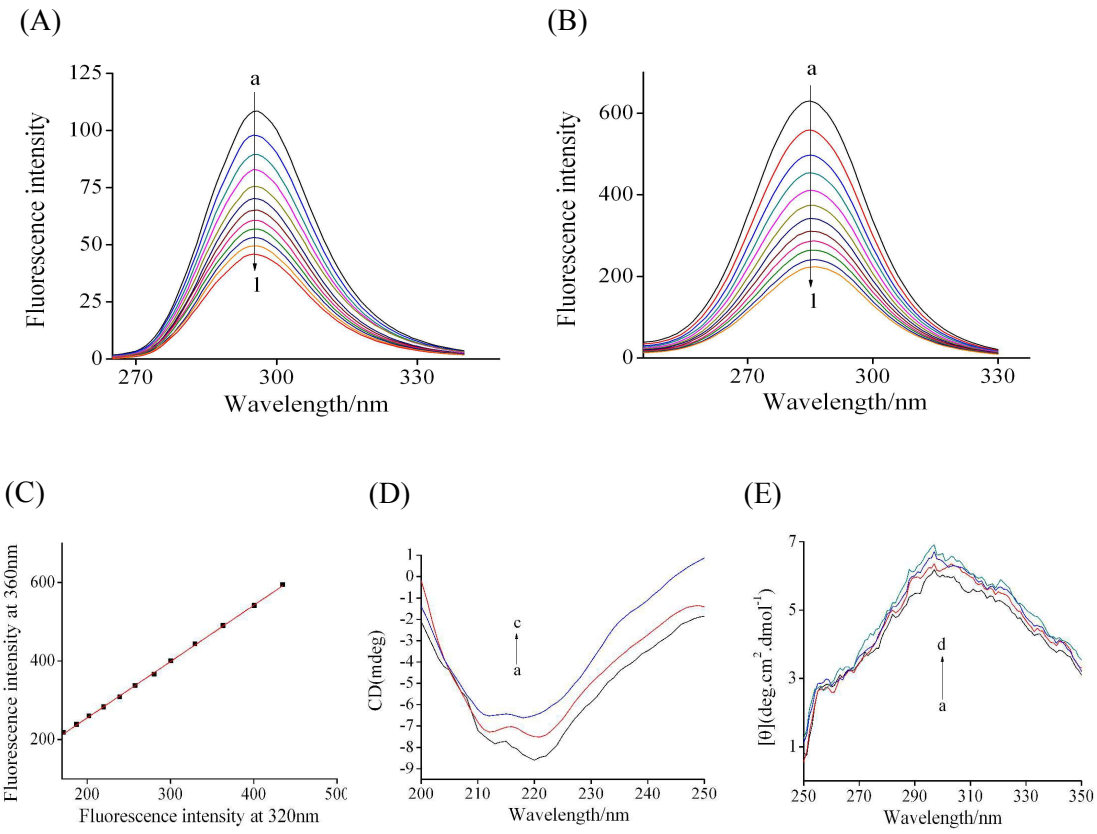

Fig. 4.

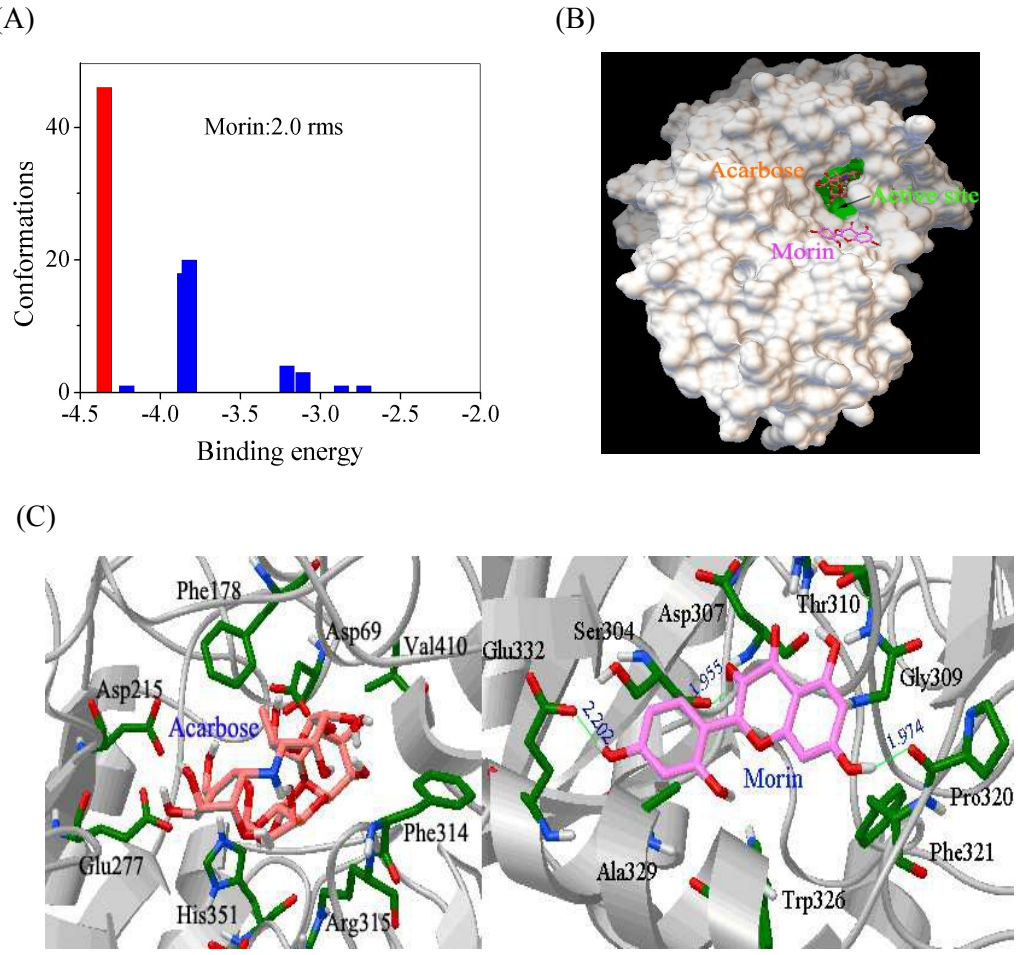

Graphical Abstract

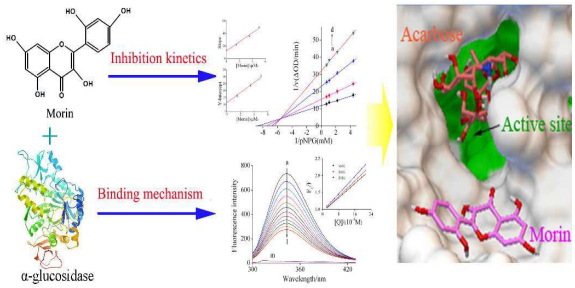

Text:

Morin can inhibit the activity of α-glucosidase and attenuate the generation of AGEs both related to diabetes mellitus.